Dynamics of Mobile Ions: Fitting of CKN Frequency Response Data without an Excess Wing

ARTICLE *in* THE JOURNAL OF PHYSICAL CHEMISTRY B · JULY 2007

Impact Factor: 3.3 · DOI: 10.1021/jp068470o · Source: PubMed

1 AUTHOR:

James Macdonald
University of North Carolina at Chapel Hill
203 PUBLICATIONS **7,844** CITATIONS

Dynamics of Mobile Ions: Fitting of CKN Frequency Response Data without an Excess Wing

J. Ross Macdonald*

Department of Physics and Astronomy, University of North Carolina, Chapel Hill, North Carolina 27599-3255

Received: December 9, 2006; In Final Form: March 19, 2007

Ion dynamics effects and the resulting dispersed frequency response of conducting materials have often been explained in the past by a combination of the Moynihan original modulus formalism (OMF) and the Ngai coupling model (NCM). These incorrect approaches and their inappropriate conclusions are replaced by alternate, Kohlrausch-related physically reasonable conductive-system fitting and interpretation models that are then used for the analysis of both limited-range and wide-range data for the supercooled liquid $0.4Ca(NO_3)_2 \bullet 0.6KNO_3$ (CKN). Detailed analysis of the limited-range 342 K data at the electric modulus immittance level shows that OMF fitting leads to an excess wing and that more appropriate models fit the data well without such a wing. Further, although such models allow estimation of the bulk dipolar dielectric constant of the material, as well as one associated only with mobile charges, they lead to implausibly small estimates of the important Kohlrausch K1 model shape parameter, β_1, and lead to an inadequate determination of its characteristic relaxation time. Therefore, wide-range CKN data sets extending to nearly 10^{12} Hz for the temperatures 342, 350, 356, and 361 K were very well-fitted with a more detailed composite model but one still involving K1 response. All model parameters were well-determined with no excess wings; β_1 estimates were all much closer to the universal value of 1/3; and the estimated model parameters led to a Boson peak beyond 10^{12} Hz, to very large thermal activation energies, and to evidence that the mobile charge concentration reached a saturation value at about 356 K. Such results do not support assumptions about variable ion−ion correlation, a mainstay of the OMF and NCM approaches. Finally, it is shown that although excess wings can sometimes be eliminated by using just an appropriate bulk fitting model and series blocking-electrode capacitor, as shown for the present narrow-range data, adequate fitting of the present wide-range data sets over their full spans of as much as 13 decades required the addition of an additional series dispersive-response model to the composite model. This addition seems likely to be required to take adequate account of the presence of more than one species of mobile charge in CKN.

1. Introduction

Ngai et al.[1] published an article entitled "Comparison of Dynamics of Ions in Ionically Conducting Materials and Dynamics of Glass-Forming Substances: Remarkable Similarities." Another paper[2] (one of the authors is also an author of ref 1) is closely related, since both deal with cooperativity in ion dynamics associated with ion−ion correlations. Both of their data analyses use the 1973 original modulus formalism (OMF) of Moynihan et al.[3] to obtain estimates of a shape parameter, $\beta \equiv 1 - n$, with n being a measure of the width of conductive-system $M''(\omega)$ peaked frequency domain response. Estimates of β shape parameter values, when derived from OMF fits, have been found in hundreds of publications over the last 30 years to increase toward unity with increasing temperature or with decreasing mobile-charge concentration. Through the aegis of the Ngai coupling model (NCM),[4] such β variation is then interpreted as a measure of ion−ion correlation, with no correlation remaining in the $\beta = 1$ and $n = 0$ limits. A list of acronym definitions is included at the end of this work.

The above procedure seems both plausible and consistent. Unfortunately, it is neither, and the association between variation of the OMF β and correlation and cooperativity is unsupported for conductive-system dispersive behavior because of a crucial error in the OMF approach, one discussed in the next section. Thus, the OMF should be replaced by a corrected model, for example, the important corrected modulus formalism (CMF) discussed in section 2. The failure by users of the OMF and NCM to refer to earlier work that discusses the defects of these response models [e.g., refs 5−11] deprives readers, editors, and referees, who may be unaware of the criticisms and inappropriateness of these approaches, of a balanced picture of the situation and may lead to continued use of faulty procedures and of their incorrect implications.

In the present work, detailed analysis will be presented of isothermal dispersed frequency-response data for $0.4Ca(NO_3)_2 \bullet 0.6KNO_3$ (CKN) at temperatures of 342, 350, 356, and 361 K. For the 342 K data set, the results are compared with those of ref 1 for the same data. Special attention is devoted to comparing approaches that fit well the high-frequency wing of the $M''(\nu)$ data with those that do not and thus leave an excess wing to be explained by the invocation of further physical processes, which is proposed in refs 1 and 2 but not actually used there to fit data in the excess wing region.

In order to allow a comparison of fitting possibilities and results for both narrow and wide frequency ranges, data involving several different frequency ranges are employed : $6 < \nu < 10^6$ Hz for the 342 K data, $20 \leq \nu \leq 10^9$ Hz for the 350 and 356 K data sets, $0.03 < \nu < 10^{12}$ Hz for the 342 K

* Phone: 919-967-5005. E-mail: macd@email.unc.edu.

10.1021/jp068470o CCC: $37.00
Published on Web 05/27/2007

data set, and $20 \leq \nu < 10^{12}$ Hz for the 361 K one. The smaller 342 K set, called NW for narrow window hereafter, was cut off at both ends and is used for initial analysis. The 350 and 356 K sets were not cut off but do not extend as far into the high-frequency region as do the 342 and 361 K ones. The full four data sets will be designated hereafter by WW, for wide window.

After a discussion of fitting models in section 2, the next two sections present detailed fitting results and excess wing discussion for the NW data set. Section 5 compares excess wing and better fitting results for the NW and WW CKN data sets and for some other materials, and section 6 is a summary of the results.

2. Data Analysis Approaches

2.1. Kohlrausch-Related Models. The ref 1 authors state that their CKN fit lines are "...the high-frequency part of the Fourier transform of the Kohlrausch fit to the same data expressed at the electric modulus, M^*, and transforming the obtained fit to ϵ''." More explicitly, the Kohlrausch fit that they mention involves transformation of stretched-exponential (SE) temporal response: $\phi(t) \equiv \exp[-(t/\tau)^{\beta}]$, to the frequency domain, where τ is the characteristic relaxation time of dispersed response and β is its shape parameter, with $0 < \beta \leq 1$. Their fits of the 342 K frequency-response data led to a τ estimate of 6.6×10^{-4} s, and they list β estimates of both 0.66 and 0.67.

The above description of the fit model used in ref 1 is ambiguous and thus requires clarification because users of the OMF and NCM approaches have not generally distinguished between two different but closely related conductive-system Kohlrausch frequency-response models, K0 and K1.[11] These models were originally designated KWW0 and KWW1[12] and also as CSD0 and CSD1, respectively.[6] No such overt model distinctions appear in publications using the OMF and NCM fitting models. All models are most appropriate for materials with mobile charge of a single species.

The one-sided Fourier transform of the $\phi(t)$ correlation function leads, for conductive-system situations, to a normalized expression for the complex resistivity frequency response,[8,11]

$$I_k(\omega) = I'_k(\omega) + \mathrm{i}I''_k(\omega) = \int_0^{\infty} \exp(-\mathrm{i}\omega t)\left(-\frac{\mathrm{d}\phi_k(t)}{\mathrm{d}t}\right)\mathrm{d}t \tag{1}$$

where the index k is set to zero to identify the K0 model. When $I_0(\omega)$ is unnormalized and transformed from the resistivity level to the complex electric modulus level, one obtains an expression for the K0 response model,

$$M_{C0}(\omega) = \mathrm{i}\omega\epsilon_V\rho_{C0}(\omega) = \mathrm{i}\omega\epsilon_V\rho_0 I_0(\omega) \tag{2}$$

where the C subscript indicates a conductive-system situation, ϵ_V is the permittivity of vacuum, and ρ_0 is the direct current resistivity. When used as a fitting model, the K0 involves the free parameters $\rho_0 \equiv 1/\sigma_0$, τ_0, and β_0, where τ_0 is the characteristic relaxation time of stretched-exponential temporal response and β_0 is its shape parameter.

In spite of the model description in ref 1, the K0 is not the model its authors actually used for their CKN analyses, as verified herein by data fitting comparisons. Instead, they used the OMF K1 model[3] calculated from the $I_0(\omega)$ expression of eq 1 by

$$M_{C1}(\omega) = M'_{C1}(\omega) + \mathrm{i}M''_{C1}(\omega) \equiv \mathrm{i}\omega\epsilon_V\rho_0 I_1(\omega) \equiv [1 - I_{01}(\omega)]/\epsilon_Z \tag{3}$$

where the 01 subscript indicates that $I_{01}(\omega)$ function is of the form of $I_0(\omega)$ but involves the $k = 1$ shape parameter, β_1, rather than that of the K0 model, β_0.[8,11] Although there are no closed-form expressions for the K0 and K1 models for arbitrary values of their shape parameters, their responses may be accurately calculated to five or more significant figures for data fitting, simulation, or inversion using the free LEVM complex nonlinear least-squares program.[13]

The K1 model parameters are ρ_0, τ_0, and β_1. When fitting the same data with the K0 or K1 models, their parameter estimates, especially those of τ_0 and β_1, are quite different. The β_1 shape parameter is just designated as β in OMF/NCM treatments using the K1 model. It is important to note that the K1 model is the only CSD one that has been derived from both macroscopic[3] and microscopic approaches,[14,15] as shown in refs 11, 14, and 15. Not only is it thus unique but in addition and most importantly it has been found to fit frequency-response data for a wide variety of materials involving charge carriers of a single species, as discussed below.

2.2. Disparate Limiting Dielectric Constants and Composite Fitting Models. The names of the composite fitting models considered here include three elements in the form CBS, where C represents an ideal capacitance in parallel with B; B denotes a bulk dispersion response model; and S designates a model representing electrode polarization effects, in series with CB. In the present NW work, it is found sufficient to take S as an ideal blocking capacitance. The name of the most important composite model employed herein is thus CK1S.

The important dielectric-constant quantity $\epsilon_Z \equiv 1/M'_{C1}(\infty)$ of eq 3 is not the same for the OMF and the CMF K1 models. The crucial difference between these models is that OMF fitting one involves only the K1 while the CMF approach involves not only the K1 but also a separate capacitance in parallel with it, one whose equivalent dielectric constant, $\epsilon_{D\infty}$, is the endemic high-frequency-limiting bulk dielectric constant associated with induced and permanent dipoles and possibly higher multipoles in the material.

The resulting composite model is named the CK1, and data fitting with this model yields estimates not only of the K1 parameters but also of $\epsilon_{D\infty}$. Further, here, $\epsilon_Z = \epsilon'_{C1}(\infty) \equiv \epsilon_{C1\infty}$, a nonzero high-frequency-limiting dielectric quantity involving effective dipoles induced by vibratory motion of mobile charges in potential wells. In ref 15, it is shown how this quantity may be derived from the results of the 1973 microscopic treatment of Scher and Lax.[14] This continuous-time, random-walk model has recently been termed both "paradigmatic" and "standard" by Phillips,[16] but it only leads to the K1 model when its general waiting time distribution, $\phi(t)$, is taken to be a stretched exponential and its high-frequency response is properly extended.[15]

In contrast, for the K0 model, $\epsilon'_{C0}(\infty) = 0$, and this model alone thus yields no peak in $M''_{C0}(\omega)$, inconsistent with experiment. But the CK0 model does lead to such a peak. For this composite model, the dielectric constant associated with the parallel capacitance, ϵ_∞, is the full high-frequency-limiting effective dielectric constant of the material.

For the CK1 model, there are two disparate contributions to ϵ_∞, monopolar and dipolar, so $\epsilon_\infty = \epsilon_{C1\infty} + \epsilon_{D\infty}$. The one that is conductive-system monopolar, $\epsilon_{C1\infty}$, may be expressed as[5,8,11,12,15]

$$\epsilon_Z = \epsilon_{C1\infty} = (\sigma_0\tau_0/\epsilon_V)\langle x\rangle_{01} = \epsilon_{Ma}\beta_1^{-1}\Gamma(\beta_1^{-1}) \tag{4}$$

where the Maxwell quantity ϵ_{Ma} is defined as $\sigma_0\tau_0/\epsilon_V$, $\langle x\rangle_{01}$ is the mean of $x \equiv \tau/\tau_0$ over the K0 distribution of relaxation times

TABLE 1: Fitting Results for Narrow-Frequency-Range CKN Data at 342 K[a]

#, model	level	$100S_F$	$10^{-9}\rho_0$ (Ω-cm)	τ_0 or τ_{0M} (s)	β_0, β_1, or β_{1M}	$\epsilon_{C1\infty}$ or ϵ_{OMF}	$\epsilon_{D\infty}$	ϵ_∞
1 CK0	M	25.8	1.58	6.6×10^{-4} F	0.665 F			8.64
2 K1	M	27.7	1.35	6.6×10^{-4} F	0.665 F	7.37		7.37
3 K1	M-U		1.27	6.68×10^{-4}	0.669	8.19		8.19
4 K1	M-P	15.2	1.60	6.13×10^{-4}	0.526	7.93		7.93
5 K1S	M	9.08	1.38	5.65×10^{-4}	0.552	7.81		7.81
6 CK1	M	10.4	1.69	$[6.71 \times 10^{-9}]$	0.158	0.062	7.64	7.70
7 CUNS	M	7.21	1.32	1.60×10^{-5}	1/3 F	0.822	6.89	7.71
8 CUNS	M-13	5.27	1.40	1.81×10^{-5}	1/3 F	0.877	6.63	7.51
9 CK0S	M	6.97	1.34	5.28×10^{-4}	0.518			7.76
10 CK0S	M-13	2.58	1.44	6.22×10^{-4}	0.477			7.63
11 CK1S	M	5.39	1.45	$[2.58 \times 10^{-8}]$	0.176	0.079	7.54	7.62
12 CK1S	M-13	2.24	1.51	$[2.35 \times 10^{-8}]$	0.175	0.074	7.39	7.46
13 CK1S	σ	6.04	1.47	$[8.52 \times 10^{-7}]$	0.230	0.270	7.36	7.63
14 CK1S	σ-13	2.23	1.55	$[3.54 \times 10^{-8}]$	0.179	0.088	7.36	7.44
15 K1S	σ'	6.81	1.37	$[2.72 \times 10^{-6}]$	0.263	0.404		
16 K1S	σ'-13	2.43	1.52	$[3.22 \times 10^{-8}]$	0.178	0.083		
17 K1	σ'	7.30	1.56	$[5.03 \times 10^{-7}]$	0.217	0.226		
18 K1	σ'-13	2.67	1.65	$[5.28 \times 10^{-9}]$	0.157	0.050		
19 CK1	M″	2.58	1.57	$[5.85 \times 10^{-9}]$	0.159	0.050	7.42	7.47
20 CK1	M″-13	2.30	1.58	$[5.73 \times 10^{-9}]$	0.160	0.048	7.38	7.43

[a] Here level designates the level and type of the data fitted. Parameter estimates enclosed in brackets [] have relative standard deviations of 0.5 or greater. The symbol S, as in K1S, indicates the presence in the fitting model of a series blocking specific capacitance of the order of 10^{-10} F/cm, while C, as in CK1, designates a parallel specific capacitance leading to the dielectric constant estimates in the $\epsilon_{D\infty}$ column. The F symbol indicates that a parameter value is fixed. All fit results used proportional weighting (P), except that indicated with U, unity weighting. All fits involved 17 data points except those marked 13, where the three highest frequency values and one outlying lower value were omitted. K1 and K1S models are of OMF character and involve τ_{0M} and β_{1M} parameters.

involving the CK1 fit value of β_1, and Γ is the Euler gamma function. Note that these averages equal 1, 6, and 720 for β_1 values of 1, 1/3, and 1/6, respectively. CK1-model fitting yields estimates of $\epsilon_{D\infty}$ and the parameters of eq 4, allowing the calculation of the corresponding value of $\epsilon_{C1\infty}$, not a separate fitting parameter in the LEVM program.

For the OMF, ϵ_Z was originally defined as $\epsilon_{D\infty}$.[3] Since no other contributions to the full high-frequency-limiting dielectric constant, ϵ_∞, are recognized in the OMF approach, ϵ_Z is now usually identified as ϵ_∞ for this model. In order to allow ready identification of OMF parameters, a subscript M (for Moynihan) will be added to their designations hereafter. Then the OMF-K1 approach leads to

$$\epsilon_Z = \epsilon_{OMF} \equiv (\sigma_{0M}\tau_{0M}/\epsilon_V)\langle x\rangle_{01M} = \epsilon_{MaM}\beta_{1M}{}^{-1}\Gamma(\beta_{1M}{}^{-1}) \quad (5)$$

where $\epsilon_{MaM} \equiv \sigma_{0M}\tau_{0M}/\epsilon_V$. One expects only small differences between the fit estimates of σ_0 and σ_{0M}. Like $\epsilon_{C1\infty}$, ϵ_{OMF} is a calculated quantity but not solely a conductive-system one.

The above results show that fits of a data set with the CK1 model allow values of both $\epsilon_{C1\infty}$ and $\epsilon_{D\infty}$ to be separately estimated, while the CK0 and OMF-K1 model fits yield estimates of only their sum, ϵ_∞. In the majority of cases, the CK1 leads to appreciably better fits, including smaller estimates of the parameter uncertainties, than do the other two models. But note that the OMF model, a conductive-system one, derived from the SE $\phi_0(t)$ conductive-system correlation function,[3,15] nevertheless, directly involves through eqs 3 and 5, the eq 5 $\epsilon_Z = \epsilon_\infty$ quantity, one that implicitly but necessarily includes terms associated with both dipolar and ionic processes since it includes no separate fitting parameter representing $\epsilon_{D\infty}$. It is clearly inappropriate for a purely conductive-system model to directly involve purely dipolar effects through $\epsilon_{D\infty}$.

This theoretical inconsistency[7] leads to the experimentally observed fact that K1 fitting parameters estimated from fits of data at all immittance levels except those at the σ' and ϵ'' levels, where $\epsilon_{D\infty}$ plays no role, depend on the value of $\epsilon_{D\infty}$. In contrast, CK1 complex or separate-part fits at all immittance levels yield closely the same K1 parameter estimates independent of $\epsilon_{D\infty}$, provided that a good fit is present for any level. Thus, for example, OMF fits of $M(\nu)$ or $M''(\nu)$ yield very different β_{1M} estimates from those following from OMF fits at the ϵ'' level (e.g., refs 7, 8, 9, and 11). Also, as expected, CK1 and OMF-K1 β_1 and β_{1M} fit estimates are the same for this data level. The crucial inconsistency of the OMF K1 approach is avoided in both the CK0 and the CK1 composite models by including a separate fitting parameter to account for ϵ_∞ or $\epsilon_{D\infty}$.

The failure of the OMF approach does not mean that its main element, the K1 response model, is inapplicable since the CMF CK1 model properly decouples dielectric- and conductive-system processes. Further, it has also been shown that for homogeneous materials allowing charge motion in three dimensions the CK1 shape parameter, β_1, should equal 1/3, independent of temperature and ionic concentration,[8] as often found experimentally. The resulting composite model has been termed the CUN, since it seems to be quasi-universal. In contrast, the increase of β_{1M} toward unity with increasing temperature, decreasing ionic concentration, or both has been interpreted as a measure of ion−ion correlation.[1,2,4,17,18] Because of the crucial defect in the OMF approach, such β_{1M} variation is meaningless and is thus unrelated to possible ion−ion correlation.

3. Some Fitting Results and Analysis for the NW Data Set

In ref 1, Ngai et al. show isothermal $\epsilon''(\nu)$ and $M''(\nu)$ frequency responses of CKN over a temperature range of 342−361 K. In this range, CKN is a supercooled liquid with very high viscosity. Since Ngai et al. present fits of intermediate-frequency-range 342 K data only in the neighborhood of the peak of the $M''(\nu)$ response, appropriate for excess-wing analysis, I shall first analyze the same region here, all data kindly provided by Dr. Peter Lunkenheimer.[19]

Table 1 and Figures 1 and 2, which illustrate some of the fitting results presented in the table, compare the appropriateness of various fitting models, particularly for fitting data only over two limited frequency-response windows extending up to about 50 kHz and to nearly 1 MHz. Although much experimental

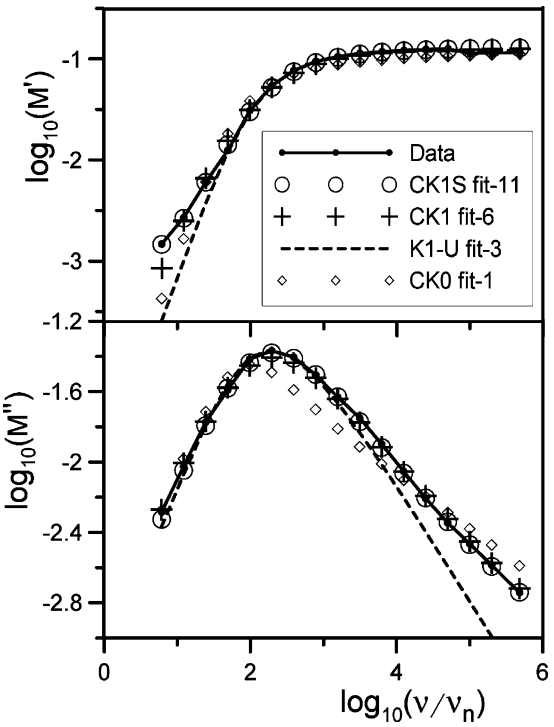

Figure 1. Log−log plots of 342 K CKN complex $M(\nu)$ NW data and the results of fitting with various conductive-system models defined in the text. Here and elsewhere, ν_n is 1 Hz. The right-hand numbers following "fit" in the caption identify the associated rows in Table 1.

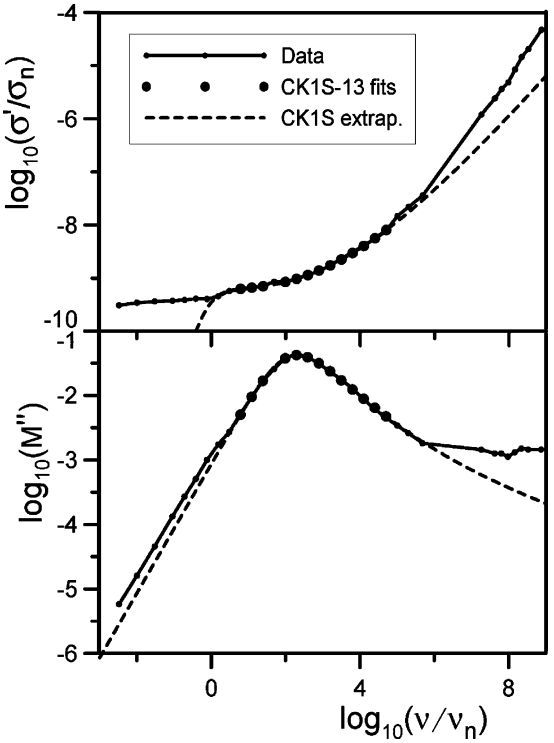

Figure 2. Log−log plots of wider-range 342 K CKN $\sigma'(\nu)$ and $M''(\nu)$ NW data sets compared with limited-range points calculated from a CK1S $M(\nu)$ fit and extrapolated as shown. Here σ_n is 1 mho/cm.

ionic-response data does not extend much beyond the latter value, some Lunkenheimer CKN data sets actually extend nearly to 1 GHz, a much wider window, and results of fitting 342−361 K data over such ranges will be discussed in section 5.2.2.

In order to resolve the question of whether the CK0 or OMF-K1 fitting model was used in ref 1 for CKN data fitting and to examine the conclusions drawn from such fitting and discussed therein, I have carried out new detailed and accurate complex nonlinear least-squares fits of the data they considered, with results shown in Figures 1 and 2 and in Table 1. The first two rows in Table 1 show CK0 and K1 fits of the limited-range complex CKN data at the $M(\nu)$ level. For these fits, the ref 1 values of τ_{0M} and the average β_{1M} were taken fixed, and the direct current conductivity parameter, ρ_0, was a free fitting variable in both fits, as was also ϵ_∞ in the CK0 fit. The quantity $100S_F$, whose values are listed in the table, is the percent relative standard deviation of a fit, calculated from its residuals. In general, values of 1 to 2% or less represent good fits, and those of 10% or more are very poor. Thus, these first two fits are exceptionally poor. Note that for all K1-model fit results shown in Table 1, the characteristic relaxation time is denoted by τ_{0M}, while τ_0 is used for all other fits with models that involve a parallel capacitor, such as CK0 and CK1.

The third row of the table shows OMF-type K1-fit results similar to those of the second row but with all parameters free and unity weighting, a weighting type that emphasizes large data values. In Figure 1, the row-1 and row-3 fits are compared to the data. Note that when a fit point symbol appears with its center very close to that of its associated data point, the fit is excellent; further, the sizes of the symbols in the graphs are unrelated to the uncertainty of each fit point.

Comparison of the row-1 and row-3 $M''(\nu)$ results with that of the fit in Figure 6 of ref 1 shows that the CK0 results are quite different, but those of the present row-3 K1-M-U result are closely similar. Thus, it is clear that, in spite of an ambiguous description, the OMF-K1 model was used for the fits of the CKN data of ref 1. The lowest-frequency $M''(\nu)$ point in Figure 1 and a plot of the $M'(\nu)$ data were not included in the Ngai CKN analyses of ref 1, so no low-frequency discrepancies appeared in their results. Note that appreciable differences in their parameter estimates do appear between the differently weighted K1-M−U and K1-M−P fit results shown in rows 3 and 4 of Table 1, an indication of inappropriate fitting models.

The low-frequency differences between data and fit points for the K1 fits suggest the need to account for the presence of electrode polarization effects. Although such effects have often been well-represented by a series constant-phase element, the SCPE,[9,20] for the present limited-range data, a series blocking capacitor yields equivalent results with one less free parameter and so has been used herein; its presence is indicated with an S, as in the K1S composite model of row 5. As shown in the table, its inclusion reduces the percentage relative standard error of the fit from 15.2% for the K1 M−P to about 9% for the K1S, slightly better than that of the CK1 fit of row 6, which, as Figure 1 shows, exhibits appreciable low-frequency discrepancies in its $M'(\nu)$ response. The row-7 and row-8 CUNS results, involving 17 and 13 data points, respectively, are better than those of the K1S but appreciably poorer than the CK0S and CK1S ones of rows 9−12. Clearly, the CUNS model is not as appropriate here as the CK0S and CK1S ones.

Note that eliminating the poorly fitting three highest frequency data points and the fourth smallest one, so that the remaining number of points becomes 13, appreciably improves the fits. Thus, on comparing the row-9 and row-10 results and the row-11 and 12 ones, one sees that the $100S_F$ values are reduced by more than a factor of 2 without much change in the estimated parameters, a good indication of an appropriate model.

However, the comparable values of $100S_F$ for the CK0S and CK1S fits raise the question of which is the more appropriate for the present data. Although the CK1S $100S_F$ values are slightly smaller than those of the CK0S, all CK1 fits of the

present data lead to very small and uncertain estimates of τ_0. For small β_1 values, where the complex plane plot of the K1-$M(\nu)$ model approaches flatness over most of its range,[11] there is a very high correlation between β_1 and τ_0 estimates, making the latter ones quite uncertain. Nevertheless, taking each τ_0 fixed and varying it in the neighborhood of its free-fit estimate showed that the latter led to the smallest $100S_F$ value and so to the best fit. Thus, the $[\tau_0]$ values shown in the table may be at least somewhat significant.

A test of whether or not errors in the data were significant for the differences between the CK0S and CK1S 13-point fit results was carried out by using the estimated parameter values of rows 10 and 12 of the table to calculate exact responses for these models. Then, these exact data sets were each fitted by the opposite model. The resulting $100S_F$ values were only slightly smaller than those in the table and the parameter estimates were all close to those shown there. In addition, the uncertainty of the row-12 τ_0 estimate was 0.74 and that obtained from fitting the exact CK0S data with the CK1S model was 0.72, showing that these large uncertainties are indeed structural. The rest of the analyses deal with K1-model fits rather than K0-model fits.

When the parameter values obtained from the CK1S-M-13 and CK1S-σ-13 fits are used to extrapolate the response range, one obtains the results shown in Figure 2, which includes all of the available 342 K CKN data except that above 10^9 Hz. The slope of the extrapolated $\sigma'(\nu)$ line in the high-frequency region, $1 - \beta_1$, is about 0.82 here, while that of the data is close to unity, nearly constant loss (NCL). Results of CSD analyses of the full-range CKN data that eliminate this discrepancy are discussed in section 5.2.

Comparison of the two CK1S-M fit parameter estimates and those of the CK1S-σ ones in the table indicates reasonable agreement, especially for the 13-point ones, another indication of an appropriate fitting model. Particularly interesting are the comparisons of the various β_1 estimates of appreciably less than 1/3. Such low-β_1 behavior suggests that the material is not mesoscopically or microscopically homogeneous for supercooled liquids such as CKN. Note that the CK1S-M-13 $\beta_1 = 0.175$ estimate is close to the row-16 K1S-σ'-13 one of 0.178, just as expected since $\epsilon_{D\infty}$ plays no role in σ' fits and its effects are properly accounted for in CMF CK1-model fitting at all levels.

Good agreement is also present between the row-18 through 20 K1-σ'-13 and the CK1 $M''(\nu)$ β_{1M} fit estimates of 0.157, 0.159, and 0.160. These results are thus all fully consistent. However, a comparison of the OMF K1-M β_{1M} estimates of 0.67 to 0.53 of rows 2 through 4 and all of the other K1 estimates listed in the table shows a high degree of inconsistency, just as found in the past for the many materials where meaningful CK1-model β_1 estimates close to or exactly equal to 1/3 are common. So even for much smaller β_1 situations, the crucial inconsistency of the OMF approach remains present.

4. Excess Wing Considerations

The same OMF fitting results of the Lunkenheimer 342 K $M''(\nu)$ and $\epsilon''(\nu)$ CKN data shown in Figures 5 and 6 of ref 1 also appear in two 2003 publications of Ngai[17] and Ngai et al.[18] These authors draw attention to the deviation of the $M''(\nu)$ fit curve from the data at frequencies above its peak, called an excess wing:[1,17] response "in excess of the fit by either the Kohlrausch function or the Davidson−Cole function".[1] This deviation also is essentially that appearing in the K1-U fit of the $M''(\nu)$ data shown in the present Figure 1, where unity weighting was used to ensure a closer fit of the model to the peak region of the data. An important part of the Ngai work on CKN and other conducting materials is the discussion and proposed physical-model explanations of excess wing response.

Since excess wings have been appearing in published work, usually without plausible physical explanation, since the 1973 original modulus formalism work,[3] they are highly significant and thus deserve more detailed attention. First, Ngai and his collaborators do not cite the earlier CKN data analysis work of Lunkenheimer and Loidl[21] where the excess wing, electrode polarization effects, and fitting in the wing region are all discussed. Further, by considering only a restricted frequency range, Ngai et al. show no data that might be associated with electrode polarization effects, as discussed in section 3 above.

In fact, Lunkenheimer and Loidl showed in 2002 that a dielectric-system Davidson−Cole fitting model provided a good fit of the 342 K CKN $M''(\nu)$ data over the same frequency range as that of the present Figure 1, thus leading to no excess wing discrepancy, in apparent contradiction to the Ngai et al. conclusion cited above. However, note that the Davidson−Cole model, whether representing conductive- or dielectric-system dispersion,[11] is somewhat empirical, and in addition, dielectric dispersion seems much less likely than does conductive-system dispersion for the thermally activated ion-conducting material CKN. Thus, the present work is concerned with the latter approach.

5. Excess-Wing Analysis Methods and Results

5.1. Fitting and Analysis of the NW Limited-Range 342 K CKN Data Set. For situations involving mobile ions and the likelihood of conductive-system dispersion, there are several different approaches to describe and possibly fit high-frequency excess wing effects. Although the presence of a complete-blocking series capacitor, as in the fit models of Table 1 with an "S" in their names, affects only low-frequency behavior, it is often desirable to replace or add to such an electrode polarization model a series constant-phase element, $\sigma_{SC} \equiv \epsilon_V A_{SC}(i\omega)^{\gamma_{SC}}$, with $0 < \gamma_{SC} \leq 2$, as mentioned in section 3.[9,20]

Such an SCPE model affects not only low-frequency but also high-frequency response, and for the latter, its series combination with just a frequency-independent dielectric constant, such as ϵ_∞, leads to log−log slopes of $\sigma'(\nu)$ of $(2 - \gamma_{SC})$ and γ_{SC}.[22] For $\delta \equiv 1 - \gamma_{SC} \ll 1$, an NCL condition, the slope thus changes from $1 + \delta$ to $1 - \delta$ as the frequency increases, where δ may be positive or negative. References 9, 11, and 20 show examples where the inclusion of an SCPE in the composite fitting model allows excellent fitting of an excess wing region, as well as associated NCL regions where the $\sigma'(\nu)$ slope is near unity. However, electrode polarization effects are not necessarily the only reason for the appearance of an excess wing.

The results in Table 1 and Figure 1 show that the CKN $M''(\nu)$ wing region is well-fitted by either the CK1S or the CK1 composite model; so for this frequency region, no series electrode-polarization function is needed. The matter is made particularly explicit by the CUN-model synthetic data results of Figures 7 and 8a of ref 11. They show that as the $r_{DC} \equiv \epsilon_{D\infty}/\epsilon_{C1\infty}$ ratio increases from 0, the $M''(\nu)$ peak region of the response progressively narrows and approaches closer and closer to a single-time-constant Debye response, followed at higher and higher frequencies by a tail involving characteristic K1 response with a limiting log−log slope of $\beta_1 = -1/3$.

Although the estimated β_1 values of the present CK1S fits are appreciably smaller than 1/3, the r_{DC} value for the row-12 CK1S-M-13 fit is close to 100, and it is the combination of the peak-region nearly-Debye response, as shown by that of the

row-3 OMF K1-M results in the table, and the high-frequency region of the Figure1 CK1 response beyond the peak that leads to excellent fitting of the wing region.

Next, it is instructive to define the basic Debye-response relaxation time associated only with $\epsilon_{D\infty}$ and ρ_0: $\tau_D \equiv \epsilon_V \epsilon_{D\infty} \rho_0$. The $\beta_1 = 1$ limit is not meaningful for the CMF,[11] but for this value, $\epsilon_{C1\infty} = \epsilon_{Ma} \equiv (\sigma_0 \tau_0 / \epsilon_V)$, with $\tau_0 \neq \tau_D$. On the other hand, when $\beta_{1M} = 1$, $\epsilon_{OMF} = \epsilon_{MaM} \equiv (\sigma_{0M} \tau_{0M} / \epsilon_V)$ with $\tau_{0M} = \tau_D$, so $\epsilon_{OMF} = \epsilon_{D\infty}$ in this limit. The ratios r_{DC} and $t_{MD} \equiv \tau_{0M}/\tau_D = \epsilon_{D0M}/\epsilon_{D\infty}$ are measures of the approach of the frequency response to Debye behavior. It is important to realize that the approach toward CK1 Debye response, for example, as ion concentration decreases toward zero, is only indirectly associated with the probable decrease in ion−ion correlation, and this limiting response is *not* the no-correlation very-high-frequency limiting Debye response of the NCM or of the more appropriate cutoff model.[10]

Since the two quite different fitting approaches discussed above have been shown to lead to excellent quantitative fits of conductive-system wing regions for different materials, it is worthwhile to see how they can be distinguished by using the above measures. For the 24 °C $Li_2O{\cdot}Al_2O_3{\cdot}2SiO_2$ (LAS) data of ref 3, where the OMF excess wing first appeared, recent CMF CUNS analysis[11] provides a good fit of the short excess wing region as well as reasonable parameter estimates, including an estimate of $\epsilon_{D\infty}$ of about 6.1. The result for r_{DC}, about 2.2, is sufficiently close to zero to show that the experimental response is dominated by that of the $\beta_1 = 1/3$ K1 model with only minor shape distortion arising from the nonzero value of $\epsilon_{D\infty}$; so for this situation, it is high-frequency electrode polarization effects that lead to a good fit of the wing-region response. On the other hand, a K1-U OMF fit of the same data led to typical excess-wing deviations, with $\beta_{1M} \cong 0.45$, $\tau_D \cong 6.6 \times 10^{-4}$ s, and $\tau_{0M} \cong 3.9 \times 10^{-4}$ s. The resulting estimate of t_{MD} was about 0.59, showing that ϵ_{D0M} was fairly close to its pure Debye limiting value of $\epsilon_{D\infty}$. However, remember that the OMF is an invalid fitting approach.

For the limited-range CKN data of Figures 1 and 2, it is clear that the M'' excess-wing region does not extend to sufficiently high frequencies to reach the limiting K1-model slope region, about −0.175 here. The actual slope reaches a value of about −0.49 and is about −0.46 at its high-frequency end, with its magnitude decreasing with increasing frequency, as shown in Figure 2. Extrapolation of the response of the model using its fit parameters shows that it is not until about $\nu = 10^{11}$ Hz that the limiting $-\beta_1$ slope is reached, although the crossover of the lower- and high-frequency slope lines occurs at $\nu \approx 3 \times 10^7$ Hz; see Figure 2 and the wide-range fit results discussed in section 5.2.2. It is this situation that makes the estimates of the CK1S τ_0 parameter so uncertain for the Table 1 fits. Nevertheless, a good fit of the data is not obtained if the K1 parameters of the model are replaced by only a Debye response: a free resistivity parameter and a free dielectric constant one in parallel (achieved, for example, by fixing β_1 and setting τ_0 to a fixed value of 10^{-30} or less). Thus, the K1 part of the composite fitting model is necessary for a good fit.

Although the present CK1S model with only a series blocking capacitor does not lead to fitting of the nearly constant-loss region of the data shown in Figure 2 for $\nu > 10^6$ Hz, addition of an SCPE power-law response function in parallel with a blocking capacitor leads to excellent fitting of the NCL region over its range of several decades. Since a series model is needed in any case to represent the low-frequency response clearly associated with electrode polarization and it is known that a SCPE can lead to significant low-frequency and high-frequency response, it is not surprising that it can well represent NCL behavior.[9,20]

It seems clear that if electrode polarization effects are present for a set of data and the modeling of the full data with an SCPE leads to good fitting of an extended NCL high-frequency region, the alternate representation of NCL response by a parallel constant-phase element, the PCPE, is then unnecessary.[9,11,23] There are, however, some low-temperature situations where it appears that a PCPE is superior to the SCPE.[9] Certainly, more experimental and fitting work is needed to see if the SCPE is always the best choice for accounting for both low-frequency and high-frequency effects or even perhaps only for low-frequency electrode polarization ones. Another possibility is illustrated in the next section.

Ngai and his collaborators do not fit the excess-wing region of the data they discuss for conductive-system situations. Instead, they only use the OMF to fit the peak of the $M''(\nu)$ responses and then invoke physical processes that they believe are appropriate for the excess wing and higher-frequency regions, all in terms of the presence or absence of ion−ion correlation effects and the NCM.[1,17,18] They propose that an extended version of the NCM leads to NCL behavior involving ions independently hopping with low probability out of asymmetric double-well potential cages. At frequencies below the onset of NCL, they define a transition region of finite range representing times where ions begin to become correlated until the "full cooperative" hopping regime of the OMF occurs at a lower frequency.[17] Further, they invoke the NCM to calculate the characteristic relaxation time for independent relaxation (Debye response in the frequency domain), a value that, surprisingly, falls within the transition region in the medium-frequency range rather than close to the usual value of about 1 ps for the conventional NCL.

Finally, it should be noted that since the present CSD fitting approach is not directly relevant to the excess wing behavior observed for nearly pure DSD dielectric glass-forming materials such as glycerol, the "remarkable similarities"[1] between their excess wings and those for ionically conducting glasses and ion-conducting supercooled liquids such as CKN are not explained by either the present approach or by the inappropriate ones of Ngai and his coauthors.

5.2. Excess-Wing Correction for Various Materials, Temperatures, and Ionic Concentrations. *5.2.1. Summary of Some Previously Published Relevant Work.* A reviewer has stated that although the author of the present work "makes a convincing case of the problems with existing models and the improvements of his model, it is not so clear that he has demonstrated this in the data." The reviewer then suggests that the model needs to be applied to more systems and to CKN data for a range of temperatures. Therefore, these matters are further addressed in this and the next section.

Comparisons were made in 2004 between the β_1 estimates following from OMF K1- and CMF CK1-model fits for several different ion-conducting glasses at different temperatures and ionic concentrations,[7] all leading to large OMF β_{1M} values dependent on both types of exogenous variables and, in contradistinction, to better-fitting CMF values all close to 1/3, the UN-model value. Similar results were found in 2002 for the material $0.88ZrO_2{\cdot}0.12Y_2O_3$ for the range 464−583 K.[23]

In addition, $M''(\omega)$ graphs for $Na_2O{\cdot}3SiO_2$ at 273 K[22] and at 321 K[24] show characteristic OMF excess-wing behavior and excellent no-wing CMF fits for these temperatures. Similar $M''(\omega)$ excess-wing graphs for $Li_2O{\cdot}Al_2O_3{\cdot}2SiO_2$ at 297 K appear

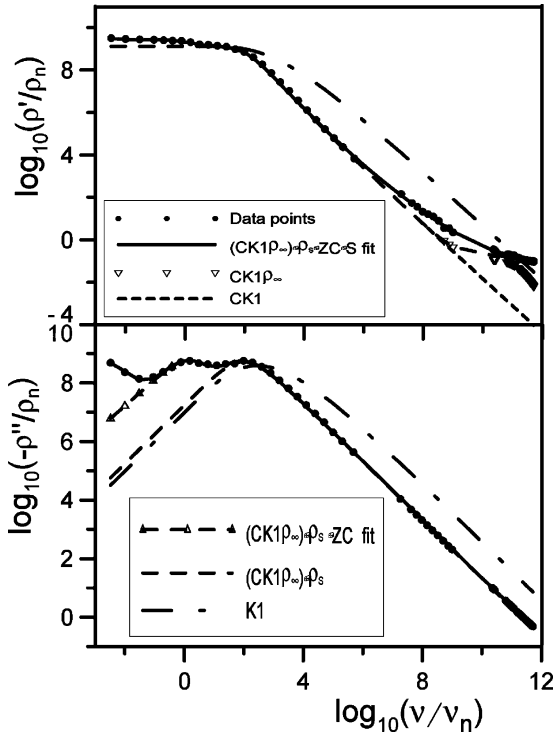

Figure 3. Log−log plots of WW 342 K CKN $\rho'(\nu)$ and $\rho''(\nu)$ data and fits and dissection results involving the responses of reduced sets of the full-fit parameter estimates. Here ρ_n is 1 ohm·cm.

in refs 11 and 25 and in ref 26 for CKN at 350 K. All of these data sets were also fitted with the CK1 or UN models and led to far better fits than the OMF ones and to β_1 values equal to 1/3 or close to it. Thus, plots demonstrating excess-wing OMF fits and no-wing excellent CMF fits for a variety of materials appear in the literature from 1997 to the present.

5.2.2. Wide-Range Fitting Results and Interpretations for the CKN WW Data Sets. Full CKN data set fittings for 342, 350, 356, and 361 K have been carried out, and pertinent results appear in Figures 3 and 4. The full fit model found to be appropriate here is denoted by $(CK1\rho_\infty)\cdot\rho_S\cdot ZC\bullet S$ and involves up to 11 possibly free parameters. The quantity in parentheses describes the K1 model with a small ρ_∞ term in series with it[15] and the combination in parallel with a capacitance C, representing the undispersed bulk dielectric constant $\epsilon_{D\infty}$. The symbol • is included here to emphasize that all quantities separated by it are in series. Here, S is a specific capacitance C_{EL} in parallel with a resistivity ρ_{EL}, both used to model low-frequency electrode polarization effects. ρ_S is a very small series resistivity, and ZC denotes Cole−Cole response at the resistivity level, $\rho_{ZC}(\omega) \equiv \rho_{ZC}/[1 + (i\omega\tau_{zc})^{\gamma_{zc}}]$.

The 342 K complex fit results are first compared here to those for the smaller data windows discussed in Table 1 and section 5.1. The 342 K data set includes 272 data points, most of them concentrated at the highest frequency region. Several different measuring devices were used to cover this 13-decade range.[19,21] Figure 3 presents 342 K data and results at the complex resistivity level because that level allows the elimination of individual series elements independently and directly. Thus, not only the data and fits are included but also the responses of parts of the full response model are shown after dissection. Such dissection is carried out by calculating the exact response associated with selected sets of the estimated parameters of the full model.

First, model response was calculated without its electrode polarization part, S, and shows that its effect is only significant

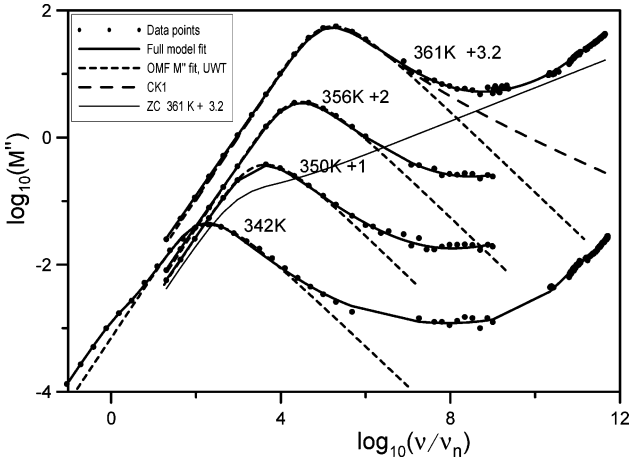

Figure 4. Log−log plots of WW CKN $M''(\nu)$ data and fits for the temperatures 342−361 K. Numbers shown after temperature identifications designate the amounts that each set of curves has been shifted upward for clarity. OMF fit results showing excess wings are included for each data set, and the 361 K results also include the CK1 and the separate ZC model response parts of the full fit.

here for the lower-frequency region of the imaginary part of the response. Then, further elimination of the ZC part of the response leads to significant changes in frequency region up to 100 Hz for the imaginary-part response and also above 10 MHz for the real part. Its absence leads to the lower decreasing response shown in the region above 10^{10} Hz. The elimination of the ρ_S and ρ_∞ elements primarily affects the highest-frequency region of the real part of the response. Finally, the figure shows very significant but well-known differences above about 100 Hz between the CK1 and the K1 contributions to the response (see, e.g., refs 7 and 11).

Although the 272-point 342 K data set contains a great many more noisy data points than does the 17-point set discussed in sections 3 and 4, its S_F value of about 0.046 is appreciably smaller than that listed in line 11 of Table 1, and as Figure 3 shows, it fits the data very closely over the full range of more than 13 decades. Further, the fit of the full data no longer leads to the essentially undefined values of τ_0 for the small-window CK1S fits listed in the table. In fact, the estimated relative standard errors of all 11 free parameters of the full fit are less than 0.1 and most are of the order of 0.01 or less. The estimated values of τ_0, β_1, $\epsilon_{C1\infty}$, and ϵ_∞ were $(3.93 \pm 0.37) \times 10^{-6}$ s, (0.276 ± 0.004), 0.471, and 8.49, respectively, all very different from, as well as more plausible than, the estimates shown in Table 1. As expected,[15] the well-estimated value of ρ_∞, about 30 ohm·cm, was very small compared with that of ρ_0 of about 1.3×10^9 ohm·cm but it nevertheless contributed usefully to the fit.

Figure 4 shows $M''(\omega)$-part data and fits following from full complex fits of the M-level data for the four temperatures shown. For clarity, results for the top three data sets and fits have been shifted upward by the amounts listed. Further, the available 350 K and 356 K data sets do not extend to as high frequencies as those of the other two sets. The ρ_S and ρ_{EL} parameters were not used for these two fits, but for the other two, ρ_S is crucially important. Its very well-defined estimated values were 0.081 and 0.049 ohm·cm for 342 and 361 K, respectively, and account for the difference between the final set of data points beginning at about 2×10^{11} Hz and the smaller-slope power-law response of the ZC shown in Figure 4 and discussed below. Further, extrapolation of the full model response to 10^{14} Hz for either temperature, as suggested by Dr. Lunkenheimer,[19] shows that inclusion of ρ_S leads to a so-called

Boson peak at about 3×10^{12} Hz and the response thereafter decreases, in agreement with data for other materials extending into this region.[19,21]

Although it is shown in ref 27 that inclusion of an SCPE in a composite CUN model can lead not only to modeling of electrode response but also to nearly zero-slope NCL response over a range of several decades, for the present data a peaked response function such as the ZC is required to model the quite evident low-frequency dispersive peak of the data in the 1 Hz region of the $-\rho''(\omega)$ 342 K results of Figure 3. Therefore, a separate electrode-polarization term is also needed. Note that the ZC dispersive response appears here as a difference at low frequencies between the full-fit results and those of the short-dash straight line. But the ZC-alone response line in Figure 4, derived from the full 361 K fit, shows that it also leads for that temperature to a high-frequency NCL slope of $1 - \gamma_{SC} \cong 0.26$, parallel to that of the data in the region from 10^9 to 10^{11} Hz.

Figure 4 also shows OMF-fit results for all four temperatures. They involved just K1-model fits of the top part of the peaked response using unity weighting and led to β_{1M} estimates of the order of 0.64. In contrast, the full-model fits led to K1 β_1 estimates ranging from 0.276 to 0.298 with an average value of 0.287. These values, quite close to 1/3, are much more plausible than those ranging from 0.16 to 0.18 for the reduced range 342 K fit results shown in Table 1, even though the latter seem to provide reasonably consistent results except for their τ_0 estimates.

One must conclude that when the frequency range is too limited on the high-frequency side beyond the main dispersion peak, which occurs for the 342 K data between 100 and 1000 Hz, K1-model β_1 estimates are suspect. The small differences between the full-model β_1 estimates and the UN-model value of 1/3 may be important here and possibly indicate conduction with an effective dimension somewhat greater than 3 or they may arise from systematic errors associated with an imperfect fitting model. It is significant, however, that the 361 K S_F value using K1 in the full model, 0.0298, only increases to 0.0306 when the UN model is used instead. Another possibility for explaining β_1 estimates less than 1/3 is discussed below.

Figure 4 includes a long-dash line calculated using only the full-model 361 K CK1 estimated parameters, a line that is necessarily curved as discussed in ref 11. Although this curve shows a smaller excess-wing than does the OMF fit in the region of nearly zero slope, 10^8 to 10^9 Hz for the present data set, it is evident that such NCL behavior arises here mostly from a combination of CK1ρ_∞ and ZC responses. This conclusion, applicable for all four CKN data sets, thus indicates that it is not only inappropriate to use the "excess-wing" nomenclature for OMF fitting results but also better to recognize that fitting with an adequate model yields no excess wing. The emphasis should be on good-fitting models, not on one such as the OMF approach that is theoretically and experimentally inappropriate.

It follows from the Nernst−Einstein equation that, when the root mean square single-hop distance is temperature independent, the $\epsilon_{C1\infty}$ effective dielectric constant of eq 4 is proportional to $\gamma N/T$, where N is the maximum mobile-charge-carrier number density and γ is the fraction of N ions that are mobile (see, e.g., refs 11 and 27). This then requires when γN is temperature-independent that for thermally activated situations ρ_0/T and τ_0 should have equal activation energies. Such energies, calculated from the present K1-model estimated values were about 3.9 and 3.6 eV, respectively, very large unequal values. The more sensitive activation energy calculated directly from fit estimates of $T\epsilon_{C1\infty}$ was about 0.23 eV with all four values or about 0.29 eV when that for the 361 K value was eliminated. Since the $T\epsilon_{C1\infty}$ values were very nearly equal for 356 and 361 K, it appears likely that γ reaches a saturated value of unity at about 356 K and decreases with decreasing temperature to a value of about 0.68 at 342 K, interesting and provocative results for a supercooled liquid and ones that deserve further extension and analysis.

In 1974, Howell et al.,[28] using the OMF approach, analyzed NW CKN data and briefly mentioned interactions of Ca^{2+}, NO_3^-, and K^+ ions, but recent molecular dynamics studies by Ribeiro[29] show that both mobile and immobile subsets of ions of all three types are present. His results also indicate that of the mobile ions NO_3^- and K^+ were most mobile and Ca^{2+} ions were least mobile, with dynamical heterogeneity present for the system. Such heterogeneity may explain the present estimated β_1 values of about 0.29 rather than the expected value of 1/3.

Dr. P. Lunkenheimer[19] has suggested to me that the two separate electrode polarization responses, modeled here by ZC and S, may be required because of the presence of two species of ions of appreciably different mobilities, with ZC modeling the partial blocking effects of the higher mobility set and S modeling that of the lower mobility ones. Nevertheless, only one CK1 hopping model is needed here for fitting the present data sets. Ribeiro's molecular dynamics results also suggest that the NO_3^- and K^+ ions may have nearly equal mobilities and are strongly correlated. If so, one might expect that only a single K1 model might be necessary as part of the composite fit model and the observed γ may increase with increasing temperature to a maximum value because of the mobilization of the originally immobile ions of either or both of these species.

6. Summary and Conclusions

Here, I summarize important characteristics of the uniquely appropriate CK1 fitting model that are verified and confirmed from many fits and interpretations such as those of the present CKN data but have not been acknowledged and discussed in previous treatments using the OMF approach. The excess wings present in the M'' and ϵ'' OMF K1 model fits of CKN data[1] are shown to be artifacts of this incorrect model, one where the data were fitted at the M level and then transformed to the ϵ'' level. The inappropriateness of the OMF model for fitting M-level data is thus inherited by the resulting ϵ'' plots, although the defect in the OMF approach does not affect individual separate σ' and ϵ'' fits, ones where the OMF and CMF K1-model approaches are equivalent because $\epsilon_{D\infty}$ plays no role in σ' and ϵ'' responses.

The following additional physicochemical insights follow from the present work: First, a crucial error in the OMF approach is shown to be the source of its nonphysical fits of the present CKN data at the electric modulus level, evidenced here by the appearance of an excess wing at the right of the peak of $M''(\nu)$ plots.[1,3] In contrast, the CK1S fitting model fits the NW data well at all immittance levels and leads to no excess $M''(\nu)$ or $\epsilon''(\nu)$ wing, thus avoiding the need for the inclusion of additional physical processes to achieve an excellent fit. For example, the introduction by Ngai and coworkers of NCM effects and their discussion of the onset of ion−ion correlation[1] are both unnecessary and nongermane to the analysis of data below the frequency region where NCL behavior begins to appear. Thus, the physically oriented processes they cite to explain their excess wings are irrelevant to the analysis of the CKN data.

The CK1 model, derived from both macroscopic and microscopic derivations, is the only one appropriate for fitting

conductive-system data with estimated shape parameter values that follow from a theoretical topological analysis involving the effective dimensionality of the ionic current path in a homogeneous medium.[8] Unlike the OMF fitting approach, it yields excellent data fits for a wide variety of materials and usually leads to estimated values of its β_1 shape parameter very close to the theoretical value of 1/3, appropriate for three dimensions. Unlike other CSD fitting models, the CK1 one leads to separate estimates of the two important contributions to the full high-frequency-limiting dielectric constant, ϵ_∞: the bulk multipole $\epsilon_{D\infty}$ one and the ionic-motion $\epsilon_{C1\infty}$ one. Such discrimination is absent from all of the hundreds of previously published OMF data analyses and is the source of their inadequacy for conductive-system data analyses.[7] It has been demonstrated that as the $\epsilon_{D\infty}/\epsilon_{C1\infty}$ ratio becomes large the peak region of the M''-(ν) data and that of the CK1 model narrows and approaches Debye relaxation behavior involving just ρ_0 and $\epsilon_{D\infty}$, and correspondingly, the dispersive contribution from the model moves to higher frequencies.

In the present supercooled-liquid case, where β_1 estimates for the NW data set are of the order of 1/6, such small values might suggest that the material may be microscopically inhomogeneous with an effective fractal dimension appreciably greater than three. However, more appropriate fits of the four WW data sets with a composite model including the CK1 and other processes, as discussed in section 5.2.2, lead to β_1 estimates quite close to the CUN model $\beta_1 = 1/3$ value.

In addition, analysis of these WW sets, unlike that of the NW one, leads to well-defined estimates of the K1 characteristic response parameter, τ_0, and when the fit model is extrapolated outside the high-frequency limit of the data, to a Boson peak. Also, different very large thermal activation energy values are estimated for ρ_0 and τ_0, strongly suggesting that the γ fraction of the maximum mobile-charge number density, N, increases with temperature until it reaches unity at about 356 K. These results convincingly demonstrate that even a reasonably consistent analysis of narrow-window data can lead to some misleading and physically inappropriate parameter estimates, and that further extension of data to appreciably higher frequencies is likely to be necessary in many situations in order to obtain meaningful estimates of all important model parameters and to shed light on the significant physicochemical processes present.

Important Acronyms and Names

CK0 A composite model involving K0 dispersive response; see section 2

CK1 A composite model involving K1 dispersive response; see section 2

$(CK1\rho_\infty)\cdot\rho_S\cdot ZC\bullet S$ Composite model defined in section 5.2.2

CKN The liquid $0.4Ca(NO_3)_2\bullet 0.6KNO_3$

CMF Corrected modulus formalism

CSD Conductive-system dispersion

CUN CK1 model with β_1 fixed at a value of 1/3; see section 2

DSD Dielectric-system dispersion

K0 Kohlrausch CSD response model; shape parameter β_0

K1 Kohlrausch-derived CSD response model; shape parameter β_1

LEVM The name of a free comprehensive data fitting and inversion program

NCL Nearly constant loss

NCM Ngai coupling model

NW, WW Narrow- and wide-window data set designations, as defined in section 1

OMF Original modulus formalism; a K1 fit model with shape parameter β_{1M}

PCPE A constant-phase-angle frequency-response element in parallel with bulk response

SCPE A series constant-phase-angle frequency-response element

SE Stretched exponential

ZC Cole−Cole model for conductive-system behavior; see section 5.2.2

Acknowledgment. I thank the reviewers for valuable suggestions and Dr. Peter Lunkenheimer for providing the CKN data used in this study and for his many valuable comments, but all of the conclusions of the present work are mine alone.

References and Notes

(1) Ngai, K. L.; Habasaki, J.; León, C.; Rivera, A. *Z. Phys. Chem.* **2005**, *219*, 47

(2) Garcia-Barriocanal, J.; Moreno, K. J.; Mendoza-Suárez, G.; Fuentes, A. F.; Santamaria, J.; León, C. *J. Non-Cryst. Solids* **2005**, *351*, 2813.

(3) Moynihan, C. T.; Boesch, L. P.; Laberge, N. L. *Phys. Chem. Glasses* **1973** *14*, 122. Moynihan, C. T. *J. Non-Cryst. Solids* **1994,** *1395*, 172−174.

(4) Ngai, K. L.; Jonscher, A. K.; White, C. T. *Nature (London*) **1979**, *277*, 185. Ngai, K. L. *Solid State Phys.* **1979**, *9*, 127. Ngai, K. L.; Tsang, K. Y. *Phys. Rev. E: Stat. Phys., Plasma, Fluids, Relat. Interdiscip. Top.* **1999**, *60*, 4511. Ngai, K. L.; León, C. *J. Non-Cryst. Solids* **2003**, *315*, 214.

(5) Macdonald, J. R. *J. Non-Cryst. Solids* **1996**, *197*, 83. Erratum: **1996**, *204*, 309. In addition, in eq A2, G_D should be G_{CD}.

(6) Macdonald, J. R. *J. Appl. Phys.* **1998**, *84*, 812.

(7) Macdonald, J. R. *J. Appl. Phys.* **2004**, *95*, 1849.

(8) Macdonald, J. R. *Phys. Rev. B* **2005**, *71*, 184307.

(9) Macdonald, J. R. *J. Phys.: Condens. Matter* **2005**, *17*, 4369.

(10) Macdonald, J. R. *Solid State Ionics* **2005**, *176*, 1961.

(11) Macdonald, J. R. *J. Phys.: Condens. Matter* **2006**, *18*, 629. On the third line of page 643 the word "imaginary" should be replaced by "real."

(12) Macdonald, J. R. *J. Non-Cryst. Solids* **1997**, *212*, 95. The symbol "sigma" should be removed from the right-hand end of eq 12 of this work.

(13) Macdonald, J. R.; Potter Jr., L. D. *Solid State Ionics* **1987**, *23*, 61. Macdonald, J. R. *J. Comput. Phys.* **2000**, *157*, 280. The newest WINDOWS version, LEVMW, of the comprehensive LEVM fitting and inversion program, may be downloaded at no cost by accessing http://jrossmacdonald-.com. It includes an extensive manual and executable and full source code. More information about LEVM is provided at this internet address.

(14) Scher, H.; Lax, M. *Phys. Rev.* **1973**, *B7*, 4491.

(15) Macdonald, J. R. *Solid State Ionics* **2002**, *150*, 263.

(16) Phillips, J. C. *J. Non-Cryst. Solids* **2006**, *352*, 4490.

(17) Ngai, K. L. *J. Phys.: Condens. Matter* **2003**, *15*, S1107. Ngai, K. L. *J. Non-Crystal. Solids* **2003**, *323*, 120.

(18) Ngai, K. L.; Habasaki, J.; Hiwatari, Y.; León, C. *J. Phys.: Condens. Matter* **2003**, *15*, S1607.

(19) Lunkenheimer, P. private communication. Lunkenheimer, P.; Pimenov, A.; Loidl, A. *Phys. Rev. Lett.* **1997**, *78*, 2995.

(20) Macdonald, J. R. *J. Non-Cryst. Solids* **2002**, *913*, 307−310.

(21) Lunkenheimer, P.; Loidl, A. In *Broadband Dielectric Spectroscopy*; Kremer, F., Schonhals, A., Eds.; Springer: Berlin, 2002. Lunkenheimer, P.; Loidl, A. *Chem. Phys.* **2002**, *284*, 205.

(22) Macdonald, J. R. *J. Chem. Phys.* **2001**, *115*, 6192.

(23) Macdonald, J. R. *J. Chem. Phys.* **2002**, *116*, 3401.

(24) Macdonald, J. R. *J. Non-Cryst. Solids* **1997**, *210*, 70.

(25) Macdonald, J. R. *J. Appl. Phys.* **2001**, *90*, 153.

(26) Macdonald, J. R.; Tuncer, E. *J. Electroanal. Chem.* **2007**, *602*, 255.

(27) Macdonald, J. R.; Ahmad, M. M. *J. Phys.: Condens. Matter* **2007**, *19*, 046215.

(28) Howell, F. S.; Bose, R. A.; Macedo, P. B.; Moynihan, C. T. *J. Phys. Chem.* **1974**, *78*, 639.

(29) Ribeiro, M. C. C. *Phys. Chem. Chem. Phys.* **2004**, *6*, 771. Ribeiro, M. C. C. *Phys. Rev. B: Solid State* **2001**, *63*, 094205.